Tellus (2000), 52A, 203–223
Printed in UK. All rights reserved

TELLUS
ISSN 0280–6495

Multidecadal climate variability in the subtropics/ mid-latitudes of the Southern Hemisphere oceans

By C. J. C. REASON, *School of Earth Sciences, University of Melbourne, Parkville, Vic., 3052, Australia; and Department of Environmental and Geographical Science, University of Cape Town, Private Bag, Rondebosch, 7701, South Africa*

(Manuscript received 9 November 1998; in final form 20 September 1999)

ABSTRACT

Observations of multidecadal variability in sea surface temperature (SST), surface air temperature and winds over the Southern Hemisphere are presented and an ocean general circulation model applied towards investigating links between the SST variability and that of the overlying atmosphere. The results suggest that the dynamical effect of the wind stress anomalies is significant mainly in the neighbourhood of the western boundary currents and their outflows across the mid-latitudes of each Southern Hemisphere basin (more so in the South Indian and South Atlantic than in the South Pacific Ocean) and in the equatorial upwelling zones. Over most of the subtropics to mid-latitudes of the Southern Hemisphere oceans, changes in net surface heat flux (particularly in latent heat) appear to be more important for the SST variability than dynamical effects. Implications of these results for modelling and understanding low frequency climate variability in the Southern Hemisphere as well as possible links with mechanisms of decadal/interdecadal variability in the Northern Hemisphere are discussed.

1. Introduction

While climate variability in the Northern Hemisphere ocean basins on decadal to multidecadal scales has been the subject of numerous studies (Deser and Blackmon, 1993; Graham, 1994; Kushnir, 1994; Trenberth and Hurrell, 1994; Latif and Barnett, 1996; Anderson and Willebrand, 1996 and references therein), far less work has been done on similar low frequency variability in the Southern Hemisphere ocean regions. A comprehensive review of the work to date on Southern Hemisphere low frequency variability, including the instrumental and proxy data available to diagnose such variability, has been provided by Jones and Allan (1998). More detailed analyses of decadal to multidecadal variability in particular regions of the Southern Hemisphere oceans during the last century have, for example, been performed by Allan and Haylock (1993) for the Australian/ Southeast Indian/Southwest Pacific Ocean region, by Allan et al. (1995) for the South Indian Ocean, Salinger et al. (1996) for the Southwest Pacific region, and by Venegas et al. (1996) for the South Atlantic. These studies have demonstrated that decadal to multidecadal variability is an important component of Southern Hemisphere climate, and that fluctuations in the locations and/or intensity of the semi-permanent subtropical anticyclones and in sea surface temperature (SST) in the western boundary currents and their zonal outflows across the southern mid-latitudes are often prominent features of the variability. The significance of variability in these western boundary current and outflow regions is that they are ones of considerable heat loss to the atmosphere; thus, SST variability here may influence mid-latitude storm tracks and hence weather and climate patterns downstream.

e-mail: cjr@egs.uct.ac.za

Attempts at understanding and modelling potential mechanisms associated with multidecadal variability in the Indian Ocean region have been made by Reason et al. (1996a). Based on the response of an ocean general circulation model (OGCM) when forced with the observed (COADS) multidecadal variability in surface winds, air temperature and derived humidity and theoretical arguments, these authors suggested that much of the observed SST variability over the Indian Ocean could have arisen through thermodynamic links between the atmosphere and the ocean, with large scale dynamical adjustment of the ocean to the winds contributing mainly in the Agulhas Current and southern mid-latitude region. An exception was the 1942–1962 period when wind stress anomalies in the southern mid-latitudes of the Indian Ocean were relatively weak but SST anomalies relatively large, and it was suggested that these might have been contributed to by changes in the Pacific winds modulating the Indonesian throughflow (Reason et al., 1996b).

To further investigate links between the multidecadal variability in Southern Hemisphere SST and that in the overlying atmosphere, the objective in this study is to analyse the response of an OGCM to observed epoch anomalies in COADS winds, air temperature and derived humidity for the tropical to mid-latitude ocean regions of the Southern Hemisphere. In so doing, it is assumed (as in many of the previous climate variability studies cited above) that wind and heat flux forcing are likely to be the most important factors in influencing the SST. The ultimate goal would be to isolate the mechanism responsible for the observed SST variability with a view to determining predictability. Given the inherent difficulties of modelling SST in global or basin scale OGCMs, which result from uncertainties in the observed fluxes and inaccuracies in the model representation of sub-grid scale physics (Giese and Cayan, 1993; WMO, 1996; Schiller et al., 1999) it is unlikely that the resulting model SST will closely match that observed. However, as a first step in investigating the SST variability, analysis of the model response to the observed epoch wind stress and heat flux forcing may enable some conclusions to be drawn concerning the processes and mechanisms likely to be important for the variability and whether these are regionally dependent. Clearly if the resulting model SST variability bears no resemblance to the observed, then this would suggest that a mechanism other than regional wind stress or atmospheric surface heat flux forcing is important (e.g., salinity/freshwater flux effects, sea–ice interactions, internal variability in the global thermohaline circulation). Furthermore, experiments that only impose either the epoch wind stress or the heat flux variability (keeping the other field at climatological values) may help to indicate which of these processes is more significant and whether this significance is spatially dependent.

Due to data limitations, only the region north of about 46°S is dealt with in any detail herein. The specific multidecadal epochs considered in this study are the same as those identified in previous observational analyses (Allan et al., 1995; Jones and Allan, 1998) and used in the modelling studies of Reason et al. (1996a,b).

2. Observations

Fig. 1, based on the GISST 2.2 data set from the United Kingdom Meteorological Office (Parker et al., 1995), shows the anomalies from the 1900–1983 annual mean SST for the various epochs after the long term global warming signal for this period has been de-trended from the data. For reference, near global plots are shown; however, only the Southern Hemisphere will be discussed in any detail. The purpose of the de-trending is to help isolate the natural multidecadal signal in the SST which is the main interest of this study. Following the suggestion of a reviewer, de-trending has been done by subtracting the first Empirical Orthogonal Function (EOF) computed over the domain of Fig. 1 from the 1900–1983 GISST 2.2 set and then computing epoch SST anomalies from the resulting data. As expected, the EOF1 pattern shows warming over almost all the domain, the exceptions being a small area of cooling in both the central subtropical North and South Pacific Oceans. EOF1 was found to account for 24% of the variance in the original data.

Inspection of Fig. 1 suggests that the multidecadal signal in SST consists of cooling throughout large areas in the Southern Hemisphere mid-latitudes (especially near the Agulhas Current retroflection and South Indian Ocean Current) and warming over most of the southern subtropics

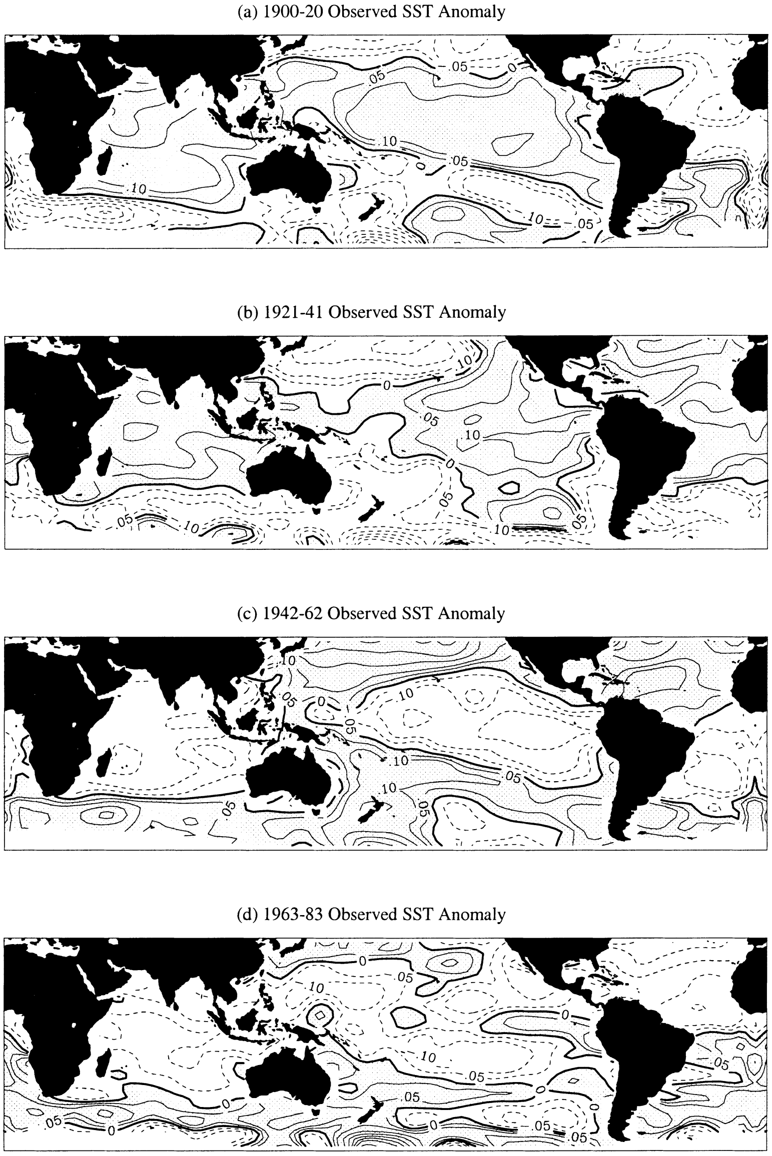

Fig. 1. SST anomalies from the UKMO GISST 2.2 1900–1983 annual mean for the (a) 1900–1920, (b) 1921–1941, (c) 1942–1962, and (d) 1963–1983 epochs. Contours are drawn at ± 0.05, 0.1, 0.2, 0.3, 0.5°C. Solid contours with stippled background denote warm anomalies and dashed contours, cool anomalies. The bold line marks the zero contour.

to tropics (except the eastern South Atlantic and parts of the western Pacific) during the 1900–1920 epoch. In the following epoch, this mid-latitude cooling weakens in the South Indian Ocean but generally strengthens in the South Pacific and South Atlantic (e.g., near the outflow from the Brazil Current and the South Atlantic Current). For the 1942–1962 epoch, the anomaly pattern is approximately the reverse of that for 1921–1941. The last epoch shows SST anomalies that are roughly opposite to those for 1900–1920 with the mid-latitude regions of western boundary current outflows again prominent. The significance of these mid-latitude regions can also be seen in the decadal epochs of SST anomalies presented in Parker et al. (1994).

Air temperature, wind speed and wind stress anomalies from the 1900–1983 COADS (Woodruff et al., 1987) annual mean are shown in Figs. 2–4 — as described later, these anomalies are used to compute anomalous fluxes to force the OGCM. The data have been interpolated from the original COADS grid to that corresponding to the model (3.2° latitude by 5.6° longitude) and a spatial filter (Hantel, 1970) applied. This procedure was also used by Allan et al. (1995) since it helps to minimize noise in the data and produce smoothed fields that are suitable for forcing the model as

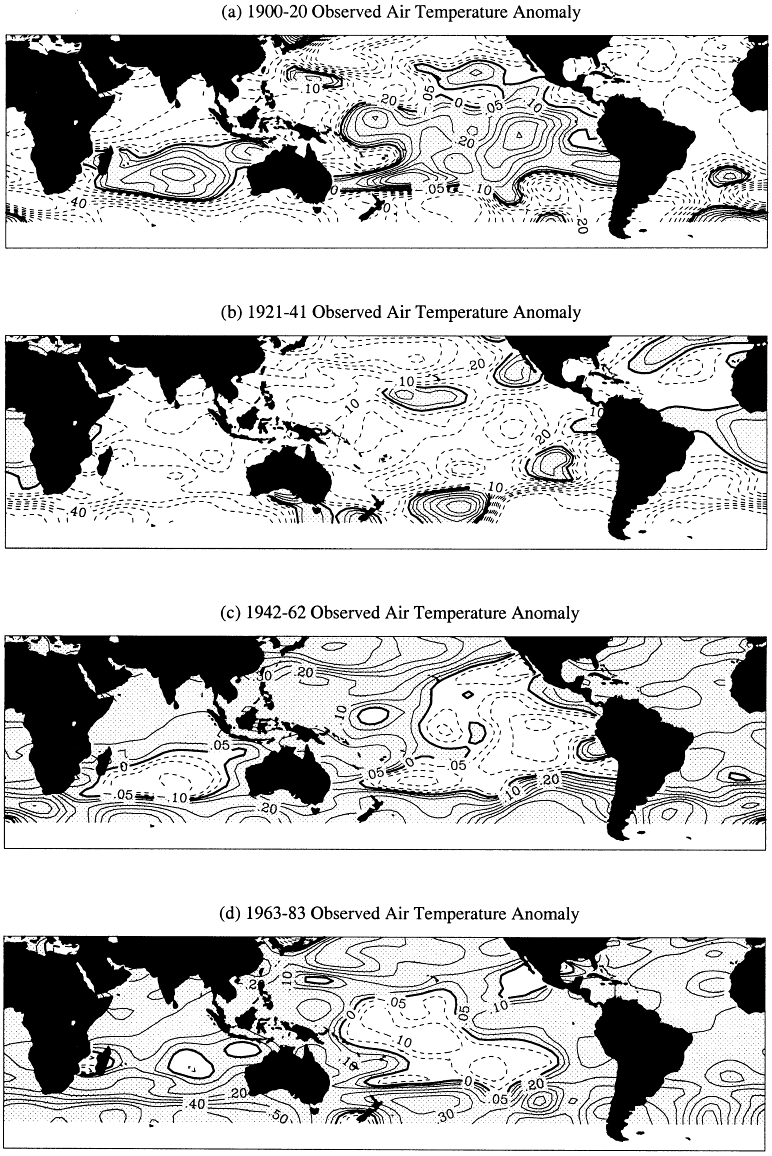

Fig. 2. As for Fig. 1 except air temperature anomalies from COADS.

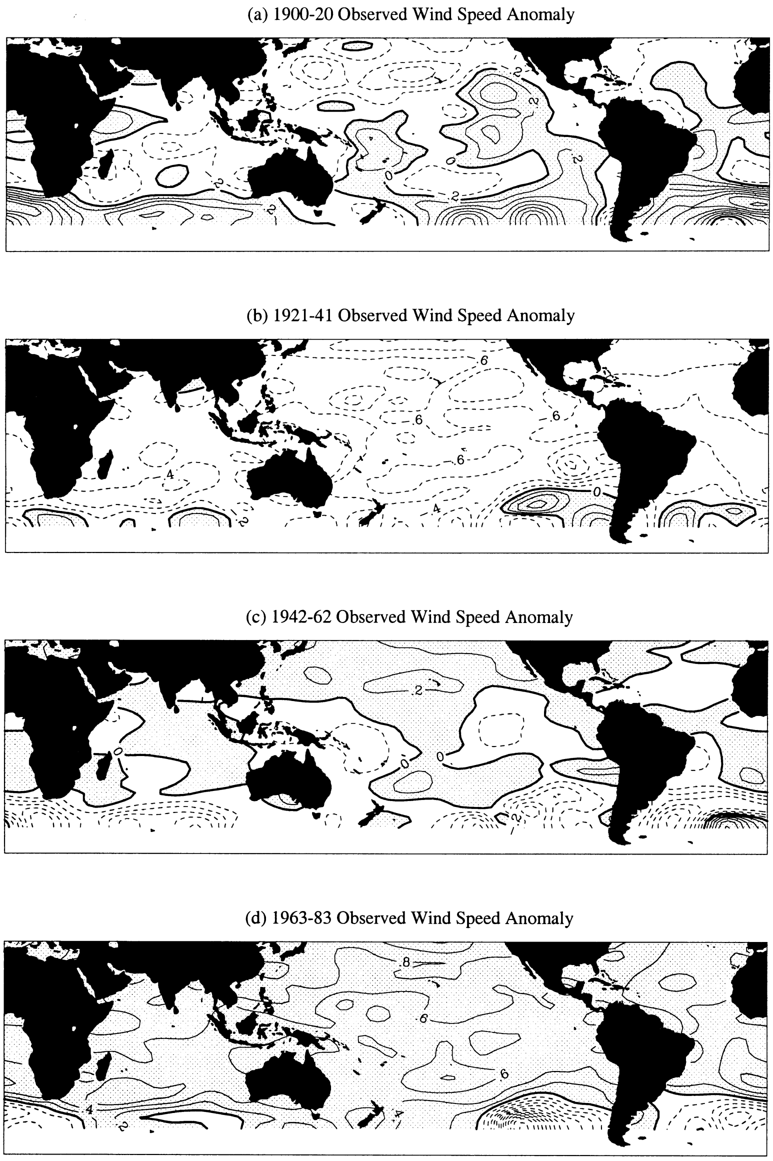

Fig. 3. As for Fig. 1 except wind speed anomalies (contour interval 0.2 m s^{-1}) from COADS.

well as being deemed preferable to trying to compute a meaningful leading EOF to remove from the data (as has been done for SST above). Air temperature anomalies (Fig. 2) tend to be of the same sign throughout the mid-latitudes of the Southern Hemisphere (cool during the first 2 epochs, warm during the last 2 epochs). Over the subtropics/tropics, much of the South Indian and South Pacific Oceans show anomalies of the same sign as each other for each epoch except 1963–1983. During the latter, it appears that the subtropical/tropical South Indian Ocean is more in phase with the South Atlantic. Wind speed anomalies (Fig. 3) are mainly negative for the Southern Hemisphere oceans during 1921–1941, except for some regions in the mid-latitudes while

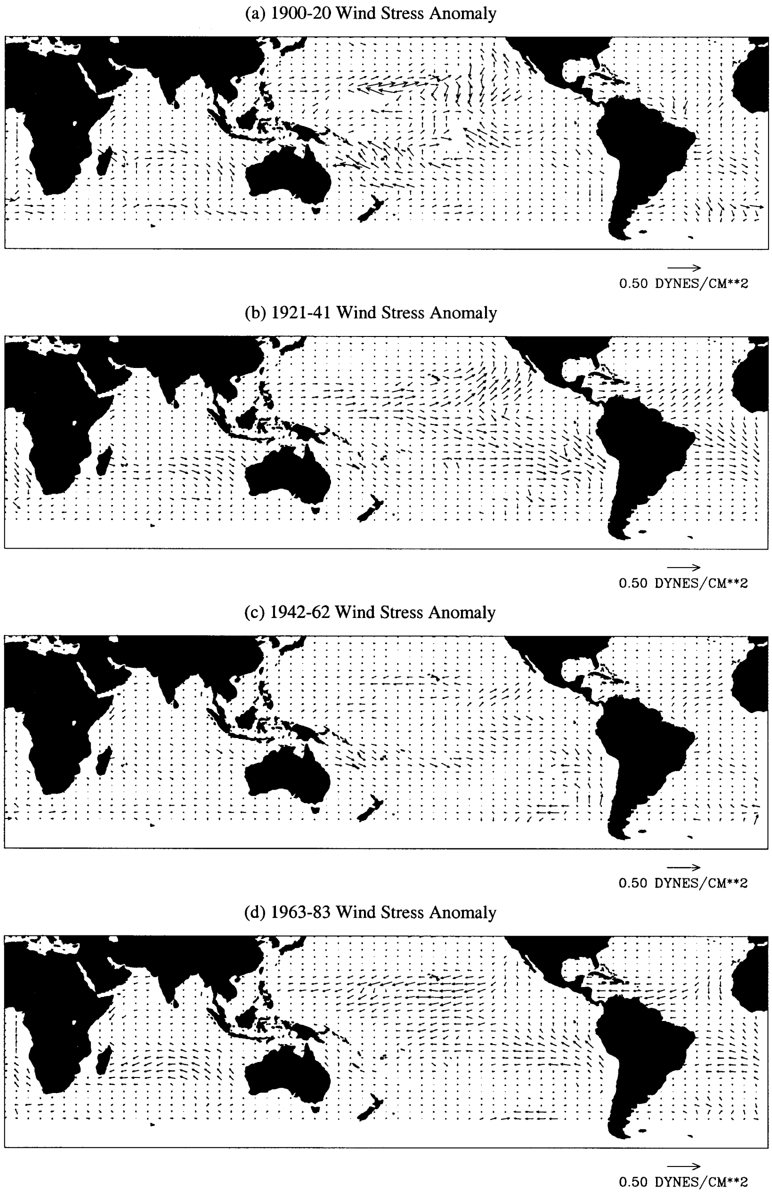

Fig. 4. As for Fig. 1 except wind stress anomalies from COADS (a scale vector is shown beneath each panel).

during 1963–1983 they tend to be the reverse. The patterns during the other epochs are a bit more complex, but during 1900–1920 are suggestive of weaker winds over most of the tropical/subtropical South Indian and central South Pacific and South Atlantic Oceans, and stronger elsewhere, and broadly the reverse of this general pattern for the 1942–1962 epoch. As with air temperature and SST, largest wind speed anomalies tend to be found either near the western boundary currents and their mid-latitude outflows or the mid-latitude southeast Pacific, or in other words, near the poleward margins of the semi-permanent subtropical anticyclones and the transition to the mid-latitude westerlies. Although there may be concerns (see Jones and Allan, 1998 for a review) with the reliability of some of the earlier epoch wind data, epoch surface pressure anomaly patterns (Reason et al., 1998) from the independent UKMO/CSIRO GMSLP2.1f (Basnett and Parker, 1997) historical global mean sea level pressure dataset are broadly consistent with the wind stress changes (Fig. 4). This increases confidence in the use of COADS winds for studies of basin to hemispheric scale decadal to multidecadal variability (cf. Ward and Hoskins, 1996).

3. Description of the ocean model and implementation of the epoch anomalies in forcing

The OGCM used here is similar to that described by Moore and Reason (1993) which was a modification of the MOM version (Pacanowski et al., 1991) of the primitive equation model of Bryan (1969) configured at CSIRO for coupling to an atmospheric GCM. An advantage of using the same OGCM configuration as that which forms part of the coupled model is that the results from the ocean only experiments performed here will provide a guide for future research into low frequency variability with the coupled model. The main differences in the OGCM compared to that of Moore and Reason (1993), and which led to improvements in the water mass climatology, are that as per Hirst and Cai (1994) the bottom topography in the North Atlantic has been slightly modified along with small changes in the Labrador and Greenland Seas to the Levitus (1982) SST and sea surface salinity used as surface boundary conditions in the model spin-up.

In terms of resolution, there are 12 levels in the vertical from the surface to a realistic bottom topography with 5 levels in the upper 215 m of the ocean. The horizontal resolution is approximately 3.2° in latitude by 5.6° in longitude over the entire world ocean, a choice motivated by the spectral R21 resolution of the atmospheric GCM. Some experiments were also performed with a model of twice the horizontal resolution (i.e., $1.6 \times 2.8°$) and vertical resolution increased to 21 levels. However, these gave similar results to the coarser resolution model while significantly increasing the computational cost and so the latter was used for the runs analysed below. In this coarser resolution model, the horizontal mixing coefficients were everywhere set to $9 \times 10^5\ \mathrm{m^2\,s^{-1}}$ for momentum and $2.5 \times 10^3\ \mathrm{m^2\,s^{-1}}$ for tracers respectively. In the vertical, these coefficients were $1 \times 10^{-4}\ \mathrm{m^2\,s^{-1}}$ except in the top 2 levels where they were increased to $2 \times 10^{-3}\ \mathrm{m^2\,s^{-1}}$ (level 1) and $1.5 \times 10^{-4}\ \mathrm{m^2\,s^{-1}}$ (level 2) so as to have some representation of the mixed layer. The implicit vertical diffusion scheme of Cox (1984) was used such that when the water column became statically unstable, the vertical diffusivity was assigned a value of $10\ \mathrm{m^2\,s^{-1}}$. The experiments described herein begin from a climatology of the Moore and Reason (1993) model forced with annual mean wind stresses from Hellerman and Rosenstein (1983). There is a restoring boundary condition on sea surface salinity (SSS) using annual mean data from Levitus (1982) with a 20 day time scale. For the surface temperature boundary condition, a heat flux Q computed as (1) is applied away from areas under sea–ice.

$$Q = R - L_{\mathrm{H}} - S_{\mathrm{H}}, \quad (1)$$

$$L_{\mathrm{H}} = \rho L C_{\mathrm{E}} |V_{\mathrm{a}}| (q_{\mathrm{s}} - q_{\mathrm{a}}), \quad (2)$$

$$S_{\mathrm{H}} = \rho c C_{\mathrm{H}} |V_{\mathrm{a}}| (SST - T_{\mathrm{a}}), \quad (3)$$

where R is the net downward radiative flux, q_{a} is the surface specific humidity, T_{a} is the surface air temperature, and $|V_{\mathrm{a}}|$ is the surface wind speed all from the Esbensen and Kushnir (1981) climatological data set for the annual mean, SST is the model sea surface temperature and q_{s} is the saturation specific humidity at this model SST given by the standard Smithsonian formula, L is the latent heat of vapourization, ρ is the density of dry air and c its specific heat, and C_{E}, C_{H} are the bulk transfer coefficients for moisture and heat, respectively. Under sea–ice, (1) is replaced by a relaxation to Levitus (1982) climatology.

From the model climatology obtained with these boundary conditions, the model was then integrated for 21 years with the observed epoch forcing for 1900–1920 imposed over the global tropical to mid-latitude region (latitudes 46°S–46°N), and climatology elsewhere. At the end of this integration, the model was integrated for further 21-year periods with forcing corresponding to the 1921–1941, 1942–1962 and 1963–1983 epochs in turn. Each integration was initialized from the end of the previous epoch.

To prevent sudden spatial changes in forcing near the boundaries of the epoch data at $\pm 46°$, the observed epoch forcing was linearly ramped towards the climatological forcing in the latitudes ± 40–$46°$. In each case, the observed epoch wind stresses were directly imposed on the momentum equation whereas the observed epoch wind speed, air temperature and derived humidity anomalies were substituted into formulae like (2) and (3) to form anomalous heat flux forcing for the various epochs. Note that since the COADS specific and relative humidity data are rather sparse and poorly sampled, particularly during the first few decades of the century, it was found preferable to use the air temperature anomalies to derive a specific humidity anomaly for each epoch by means of the standard Smithsonian formula in computing the epoch heat flux forcing. The resulting sensible and latent heat flux anomalies were of order a few $W\, m^{-2}$ and led to SST anomalies in the model that are comparable in magnitude with the observed epoch SST variability.

The above experiments included both dynamical and thermodynamic effects of the observed atmospheric variability on the ocean. To obtain an idea of the relative importance of these, two other sets of model experiments were performed. To try and isolate dynamical effects, one set only imposed the observed epoch wind stresses on the model momentum equation and kept the heat flux forcing the same as in the model climatology. The second set removed the anomalous wind stress forcing (i.e., used climatological values) and applied the epoch heat flux forcing to focus on thermodynamic effects.

As described above, only annual mean epoch forcing has been used and so seasonal effects are excluded. Although it is possible that there could be interaction between seasonal and lower frequency scales, it was found that the observed epoch wind and air temperature anomaly patterns (Figs. 1–4) were not significantly different if these were derived from seasonal as opposed to annual mean data. To test this further, an experiment was performed with seasonal effects included which resulted in little change in the model epoch solution over that under annual mean forcing but at a huge increase in computational cost. As a result, it was decided not to include seasonal effects in the experiments analysed below.

4. Model response to observed epoch variability

In this section, comparisons are made between OGCM results obtained when the model is forced with the observed epoch anomalies over the global tropics to mid-latitudes and climatology elsewhere, and with climatological values everywhere. In each case, results are presented as plots of differences between the model run with the epoch anomalies and the climatology everywhere run and discussion is focussed on the Southern Hemisphere subtropical and mid-latitude regions that are the topic of this study.

4.1. *Transport anomalies*

Fig. 5 depicts barotropic streamfunction differences for each epoch for the case when both the epoch wind stress and heat flux anomalies are applied to the model. However, as expected, the modulations to the gyre transports in Fig. 1 are little different from those induced when only the wind stress anomalies are imposed and the heat flux forcing is as in the climatology. Hence the following discussion applies to both sets of experiments. For the 1921–1941 epoch, in which there is an overall weakening of the atmospheric anticyclonic circulation over the subtropics of the Southern Hemisphere basins (Fig. 4b), there is a corresponding reduction (Fig. 5b) in the gyre transport over the South Pacific and South Indian Oceans by about 1.5–2 Sv in response to the modulated wind stresses. Over the subtropical South Atlantic, a smaller reduction of 1–1.5 Sv is apparent. The influence of the modulated Indonesian throughflow in enhancing the changes over the South Indian Ocean is evident by comparison to previous experiments by the author in which the same model was used but with epoch forcing over the Indian Ocean only, in that case the South Indian subtropical gyre was reduced by only 1 Sv under 1921–1941 epoch forcing.

Weakening of the subtropical gyre is evident only in the South Indian Ocean during the 1900–1920 epoch (Fig. 5a) with mixed signals in the other two basins reflecting the wind stress anomalies during that epoch (Fig. 4a). As a result of the mixed signal in wind stress over the Pacific, the Indonesian throughflow is only weakened by approximately 0.25 Sv which is about the

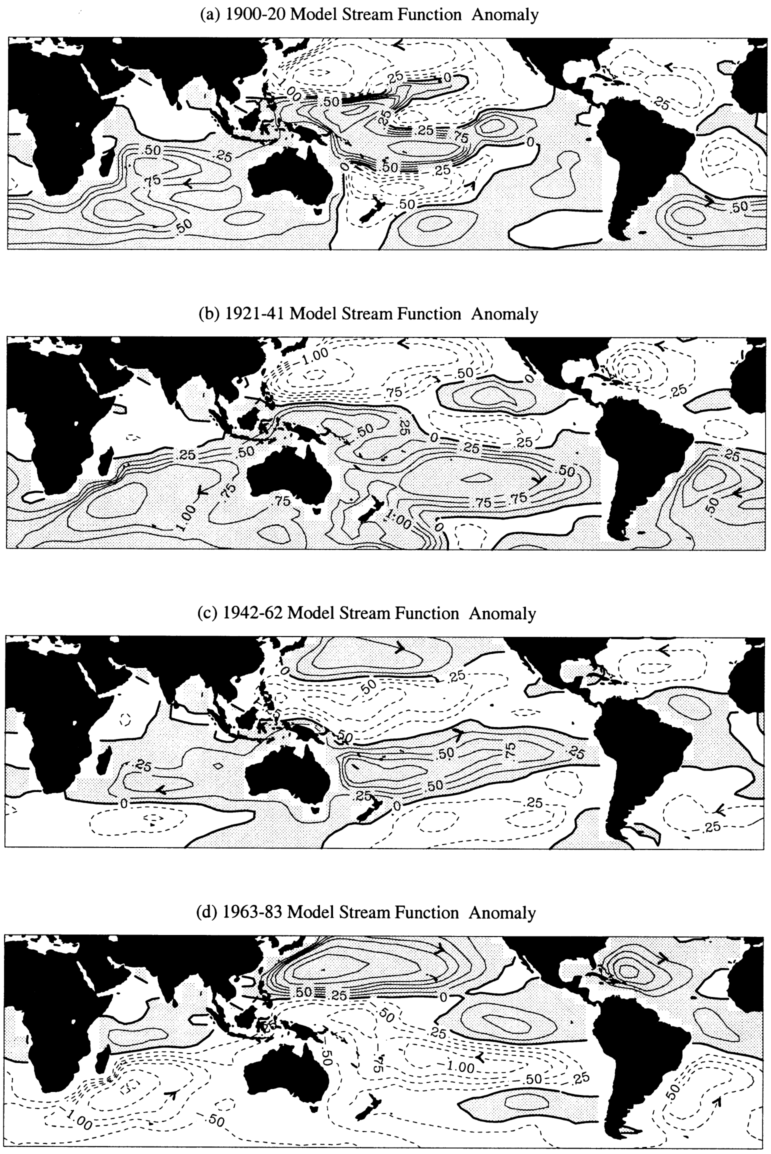

Fig. 5. Difference in model barotropic streamfunction between case when epoch wind, air temperature and derived humidity anomalies applied and climatology elsewhere and model run with climatological forcing everywhere. Panel (a) corresponds to 1900–1920 epoch, (b) to 1921–1941, (c) to 1942–1962, and (d) to 1963–1983. Contour interval is 0.25 Sv between 0 and ± 1 Sv, then ± 1.5, 2, 3 Sv. Solid on shaded background (dashed) contours indicate positive (negative) difference and the bold line marks the zero contour. The circulation sense is indicated by the arrows.

difference in anomaly magnitude over the South Indian subtropical gyre between Fig. 5a and the corresponding result when epoch forcing is only applied over the Indian Ocean.

Consistent with the 1963–1983 epoch stresses being approximately the reverse of those for 1921–1941, there is a general strengthening of the Southern Hemisphere subtropical gyres by about 1 Sv over the South Pacific and South Atlantic and by 1.5–2 Sv over the South Indian Ocean for this epoch (Fig. 5d). The latter anomalies are again enhanced by the modulated Indonesian throughflow over the Indian Ocean only result. The 1942–1962 epoch is characterised by relatively weak wind stress anomalies (Fig. 4c) and the resulting changes in transport are correspondingly small (Fig. 5c), appearing to be a transition between the 1921–1941 (Fig. 5b) and 1963–1983 (Fig. 5d) epochs. In general, Fig. 5 indicates that the most pronounced modulation of the Southern Hemisphere subtropical gyres occurs during the 1921–1941 and 1963–1983 epochs when the fluctuations in the wind stresses are most coherent.

4.2. *Temperature and heat flux anomalies*

While there are differences in detail, the model runs with both dynamical and heat flux forcing (Fig. 6) do appear to capture many of the broader features of the observed patterns in Fig. 1, particularly in the Southern Hemisphere subtropics and mid-latitude regions which are of most interest here. In the South Indian Ocean, these broad features include the tendency for warm subtropics and cool mid-latitudes during the first 2 epochs and the reverse during the last 2 epochs although the model shows a less uniform dipole signal in the subtropics than observed during 1921–1941 and to lesser extent 1942–1962. For the South Atlantic, these features include mainly cooling during 1900–1920 except warm in central region (although model underestimates the warm central area); subtropical warm, mid-latitude cool during 1921–1941; subtropical cool, mid-latitude warm during 1942–1962 (although model shows a much smaller cool area in subtropics); and mainly warm during 1963–1983. The South Pacific patterns are more complex and show various dipoles which the model has varying degrees of success at representing; the most obvious discrepancies are overestimating the areas of warming (cooling) during 1921–1941 (1963–1983). In general however, the magnitudes of the model anomalies in Fig. 6 are comparable to, or larger than, the observed and bear reasonable resemblance to the observed spatial patterns given the difficulties of modelling SST with OGCMs (Giese and Cayan, 1993; WMO, 1996; Schiller et al., 1999).

Assuming the SST anomalies to essentially have arisen from the variability in atmospheric forcing between the epochs rather than from internal ocean variability or some other mechanism, there are several processes which may be of importance in their generation and maintenance. The multidecadal time and fairly broad spatial scales of the observed SST and atmospheric variability (Figs. 1–4) suggests that large scale dynamical adjustment of the subtropical gyres (Fig. 5) to the wind stress changes (Fig. 4) and associated changes to temperature advection may contribute significantly, particularly near the Southern Hemisphere western boundary currents and their mid-latitude outflow regions (implying warming where the transport of more tropical water by the boundary current is increased as in 1963–1983 (Fig. 5d) and cooling where this transport is decreased as in 1921–1941 (Fig. 5b). Other processes of potential importance are changes in latent and sensible heat loss and upper ocean mixing driven by those in wind strength (Fig. 3), air temperature (Fig. 2) and derived humidity, upwelling changes driven either directly by the winds (Fig. 4) or as a result of changes in the convergence/divergence of horizontal currents and their interaction with the topography, changes in Ekman drift, and convection. Note that the latter would tend to occur as a result of some other induced change in SST (e.g., atmospheric heat flux, significant meridional temperature advection via Ekman drift or boundary currents).

Fig. 4 shows that the largest wind stress anomalies in the Southern Hemisphere tend to be across the 15–25°S band (i.e across approximately the same latitude range as the island of Madagascar), and in the mid-latitude central to eastern South Pacific. The sense of the relative Ekman drift in the 15–25°S band for each epoch implies SST anomalies in the subtropics of each basin that tend to be opposite to those found in the model (Fig. 6) which suggests that other processes are important here. On the other hand, the model SST variability in the South Pacific region mentioned above does appear to be in the same sense as the relative Ekman drift would imply. This suggests that changes in Ekman drift may contribute to the SST variability here along with those in surface heat flux, particularly since currents are weak in this region (north of the Antarctic Circumpolar Current). Consistent with this, the model experiment with wind stress forcing only (discussed below) did show significant SST

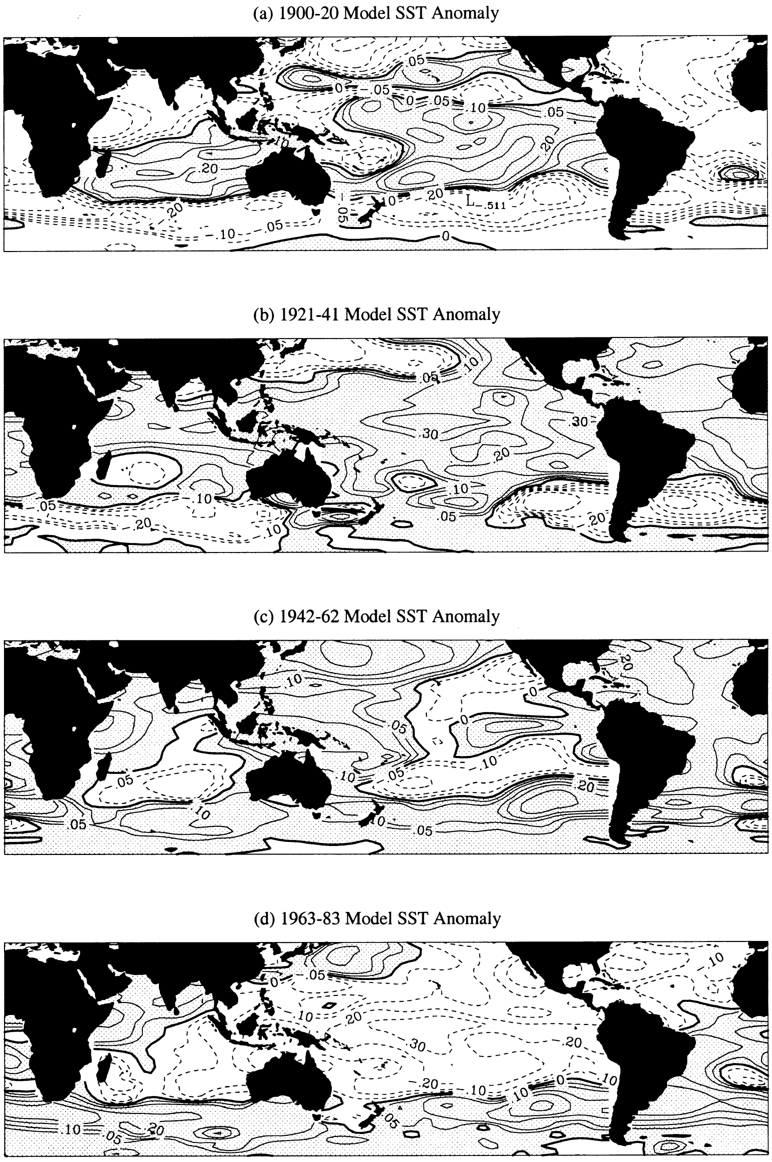

Fig. 6. As for Fig. 5 except SST. Contours are drawn at ± 0.05, 0.1, 0.2, 0.3, 0.5°C.

anomalies in the central to eastern mid-latitude South Pacific but not over much of the subtropics.

Inspection of Fig. 7, the model surface heat flux anomaly, together with Fig. 6 gives an idea of the areas in which processes other than changes in latent and sensible heat loss are likely to be important. Where the sign of the change in the epoch heat flux anomaly (Fig. 7) is opposite to that in SST (Fig. 6) and the magnitude of the former is relatively large, it is likely that a process such as dynamical modulation of the western boundary current region or of an upwelling zone is transporting water of substantially different temperature to the ambient at a rate that is rather different from the climatological case. The southern Agulhas Current and the western part of its

(a) 1900-20 Model Heat Flux Anomaly

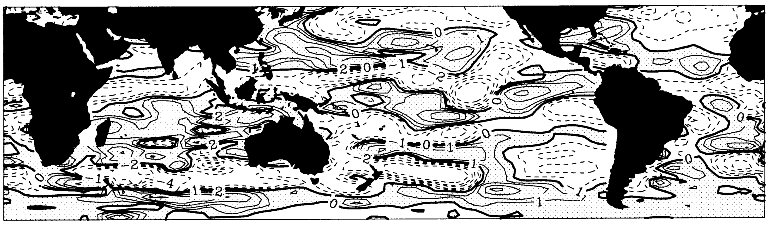

(b) 1921-41 Model Heat Flux Anomaly

(c) 1942-62 Model Heat Flux Anomaly

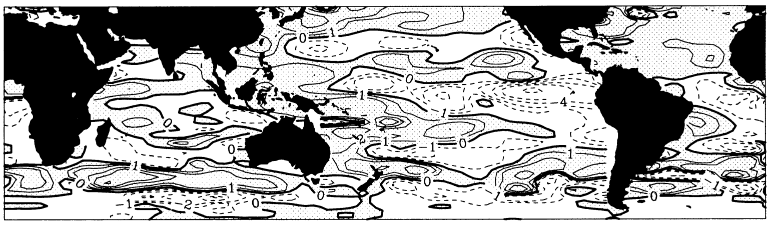

(d) 1963-83 Model Heat Flux Anomaly

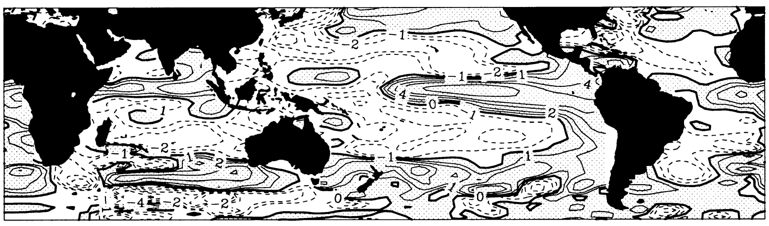

Fig. 7. As for Fig. 5 except net surface heat flux differences (solid contours on shaded background represent positive differences, and dashed negative differences). Contours are drawn at ± 1, 2, 4, 6, 10 W m^{-2} and the zero contour is bold.

outflow southeastwards into the mid-latitude South Indian Ocean provides an example of the former process during the 3 epochs of relatively large transport modulation (Figs. 5a,b,d) but not for 1942–1962, when the transport changes are small (Fig. 5c). As examples of wind-driven upwelling changes, the 1921–1941, 1942–1962 and 1963–1983 epochs show relatively large surface heat flux anomalies in the central and eastern equatorial Pacific upwelling zone (Figs. 7b–d) that are opposite in sign to the SST anomalies there (Figs. 6b–d). Examination of the model meridional overturning and vertical velocity fields (not shown) confirmed that there were significant decreases (increases) to equatorial Pacific upwelling during 1921–1941, 1942–1962 (1963–1983) and hence warm (cool) SST anomalies there (Figs. 6b–d). However, over large regions of the Southern Hemisphere subtropics, the surface heat flux anomaly is of the same sign as that in SST (Figs. 6, 7) which could occur if changes in latent and sensible heat flux are the main factor behind the SST variability in these regions. Note that there will not be an exact spatial correspondence between these subtropical heat flux and SST anomaly regions of the same sign since the horizontal currents will shift the warmed or cooled areas to some extent.

To get an indication of the direct importance of dynamical adjustment of the Southern Hemisphere subtropical gyres for the SST variability there, Fig. 6 was compared with the equivalent figure obtained when only the model momentum equation was forced with the epoch wind stresses (Fig. 4) and the heat flux forcing was kept as in the climatology. In this case, the resulting SST anomalies (not shown) were considerably smaller than those in Fig. 6 with the only significant contributions being in the dynamically sensitive areas of the equatorial upwelling regions, the central to eastern mid-latitude South Pacific (during last 3 epochs when wind stress anomalies are significant, Figs. 4b–d, and can produce Ekman drift) and the southern parts of the Southern Hemisphere western boundary currents and their mid-latitude outflows. As expected, the largest model SST anomalies were found during the 1921–1941 and 1963–1983 epochs when the wind stress variability is more coherent and organised (Figs. 4b,d) than in the other 2 epochs (Figs. 4a,c). Even in the southern parts of the western boundary currents and their outflows, the magnitude of the SST anomalies when only the momentum equation is forced is somewhat smaller (0.05–0.2°C) than in Fig. 6 (0.2–0.5°C). This result points to the significant contribution of surface heat fluxes in driving the SST variability in these boundary current regions; their contribution is not simply confined to the subtropical areas of weak mean currents as one might initially expect.

An estimate of the contribution of the heat flux anomalies to the SST epoch variability can be gained by comparing Fig. 6 to the model SST obtained when these heat flux anomalies were imposed but the wind stress forcing was kept at climatology. The resulting model SST anomalies (not shown) are very similar to Fig. 6 throughout the domain re-inforcing the importance of surface heat flux forcing for most of the Southern Hemisphere subtropics and mid-latitudes. The only obvious differences in this experiment from Fig. 6 are in the equatorial upwelling zones and in the southern western boundary current regions and their mid-latitude outflows. In the latter, the model runs with anomalous heat flux forcing only (and climatological wind stress) had pattern similar to Fig. 6 but magnitude about 50–75% of that found when both heat flux and wind stress changes are included. Note that the heat flux only and wind stress only anomalies do not necessarily linearly combine to give those shown in Fig. 6 when both types of forcing are included. The perturbation circulation induced by the wind stress anomalies advect the temperature anomalies both horizontally and vertically and this results in some areas (particularly in the outflow regions of the western boundary currents and other areas of climatological ocean surface heat loss such as the subtropical southeast Indian Ocean) being more or less prone to convection than otherwise, and hence to further changes in SST.

Based on the comparison of Fig. 6 with the epoch wind stress only and epoch heat flux only sets of experiments, it may be suggested that the contribution to the model multidecadal SST variability by dynamical effects of the wind variability (wind-driven upwelling, Ekman drift, gyre adjustment and associated temperature advection) is very small outside the equatorial upwelling zones, the mid-latitude central to eastern South Pacific, and the western boundary current regions and their mid-latitude outflows. Within these regions, dynamical effects are significant but usually not dominant over thermodynamic effects. This suggestion appears consistent with the observed multidecadal SST variability (Fig. 1) since with the exception of the mid-latitude outflow regions of the Southern Hemisphere western boundary currents and, for the last 3 epochs, the eastern equatorial Pacific, there does not appear to be any obvious evidence of tight gradients in SST anomaly aligned with the location of strong mean currents in the Southern Hemisphere.

If heat flux forcing is dominant outside the southern western boundary currents and their outflows, then it is of interest to compare the model SST anomalies (Fig. 6) with those sub-surface to get an idea of the potential contribution of vertical exchange of heat (e.g., through upwelling/downwelling motions or mixing processes). Comparison of Fig. 8, the model temperature anomalies at 370 m depth, with those at the surface (Fig. 6) suggests that there is a de-coupling over most of the tropical to subtropical South Indian and South Pacific Oceans except for the equatorial upwelling regions. As will be further discussed below, the SST anomalies over the Southern Hemisphere subtropics mainly respond to changes in heat flux forcing and do not appear sensitive to sub-surface changes. However, over significant parts of the southern mid-latitudes (particularly near the western boundary current outflows)

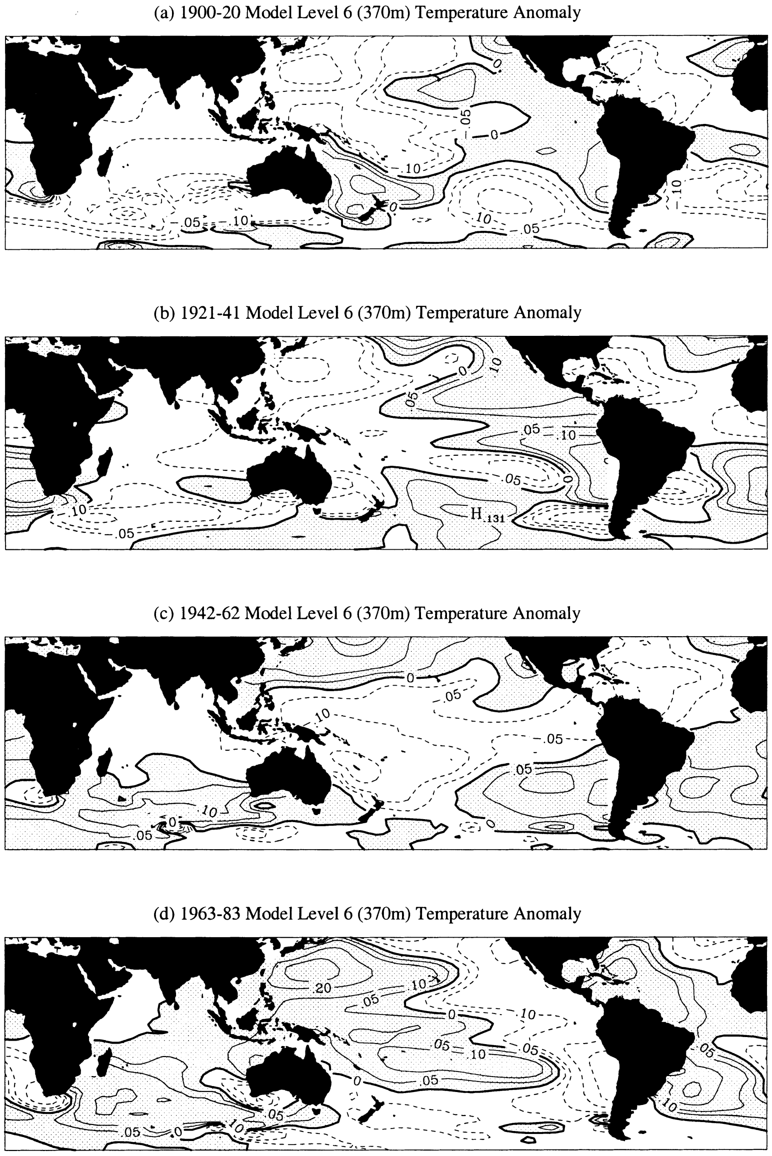

Fig. 8. As for Fig. 5 except model temperature differences at 370 m depth. Contour interval is 0.1°C except that the ±0.05°C level is also shown.

where, climatologically, the model ocean loses heat to the atmosphere and is prone to convection, the SST anomalies (Fig. 6) and those sub-surface (Fig. 8) are of the same sign indicating that there may be vertical communication of temperature anomaly. To consider this further, the model vertical velocity and meridional overturning streamfunction fields (not shown) were examined. These showed that there were significant vertical motions (mainly due to convection) in the western boundary current outflow regions where the sign of Figs. 6 and 8 tends to agree. These regions are also ones where there are significant modulations to the polewards transport of warmer tropical waters by the subtropical gyres (Figs. 5, 9) and where these are weaker (e.g., all 3 basins during 1921–1941) cool sub-surface anomalies result (Fig. 8b) and warm where these are stronger (e.g., Figs. 5d, 8d, 9d for all 3 basins during 1963–1983). Generally, the magnitude of the anomaly at depth (Fig. 8) in these mid-latitude regions is somewhat less than that at the surface reinforcing the statement made earlier that wind stress induced modulation of the gyres and associated temperature advection is only partly responsible for the SST anomalies; the epoch heat flux forcing is also important.

Further support for the importance of both dynamical modulations of the gyres and surface heat flux forcing for the SST variability in the western boundary current outflow regions comes from an estimate of the relative heat transport. Zonal sections of temperature and meridional velocity were constructed for each Southern Hemisphere basin and estimates made of the heat transport due to the modulated gyres (Fig. 5). Typical values for the epoch changes in heat transported polewards by the western boundary currents, when divided by the area of the given model western boundary current to get equivalent heat fluxes that can be "compared" with those at the surface (Fig. 7), are 0.5–2.0 W m^{-2}. In other words, the dynamical modulations of the subtropical gyre transports (Fig. 5) by the wind stresses lead to changes in heat advection in the southern western boundary current regions that are approximately equivalent to surface heat flux changes of order 1–2 W m^{-2}. This estimate may be "compared" with Fig. 7, which reflects the total surface heat flux change due to both thermodynamic and dynamical effects, and which is of order 2–4 W m^{-2} in these regions, indicating that both make significant contributions here. The eastwards extent of the mid-latitude region where dynamical effects are significant tends to be related to the climatological strength of the western boundary current. It is most obvious in the southern Agulhas Current and its outflow eastsoutheastwards across the South Indian Ocean, which is as expected given that this current is the strongest Southern Hemisphere western boundary current. Consistent with the East Australian Current and South Pacific subtropical gyre being weaker than the other two Southern Hemisphere gyres, there is a generally reduced influence of advective effects relative to thermodynamic ones in the mid-latitude South Pacific when compared with the South Atlantic and South Indian Oceans. Away from the equatorial upwelling zones and western boundary current and outflow regions, the epoch SST anomalies (Fig. 6) are linked more with surface heat exchange rather than with heat gained or lost via changes in the upwelling of sub-surface cooler waters or in the advection of heat by the currents. The relatively shallow mixed layer over the central subtropical basins, lack of convection and weaker currents tend to isolate the surface from subsurface changes (Fig. 8) in these areas and facilitate the dominance of the epoch surface heat flux forcing. Changes in this surface heat exchange arise from the observed epoch anomalies in wind, air temperature (Figs. 2–4) and derived humidity imposed on the model. It was found that most of the resulting heat flux changes arose from those in latent heat, anomalies in this flux were typically 2–3× larger than those in sensible heat. Examination of the model net surface heat flux anomalies for each epoch (Fig. 7) indicates that large regions of positive heat flux anomaly in the Southern Hemisphere subtropics (e.g., in the South Indian Ocean during 1900–1920 and the South Pacific during 1921–1941) correspond to warm SST anomalies. Conversely, the subtropics of the South Indian and South Pacific Oceans are cool during 1963–1983 when negative anomalies are apparent in the net surface heat flux (Fig. 7d). Note that the SST anomalies over the subtropics of the Southern Hemisphere basins do not correspond exactly to those in surface heat flux due to some advection by the mean or perturbation (Fig. 9) currents shifting the temperature anomalies somewhat (even though these currents are weak

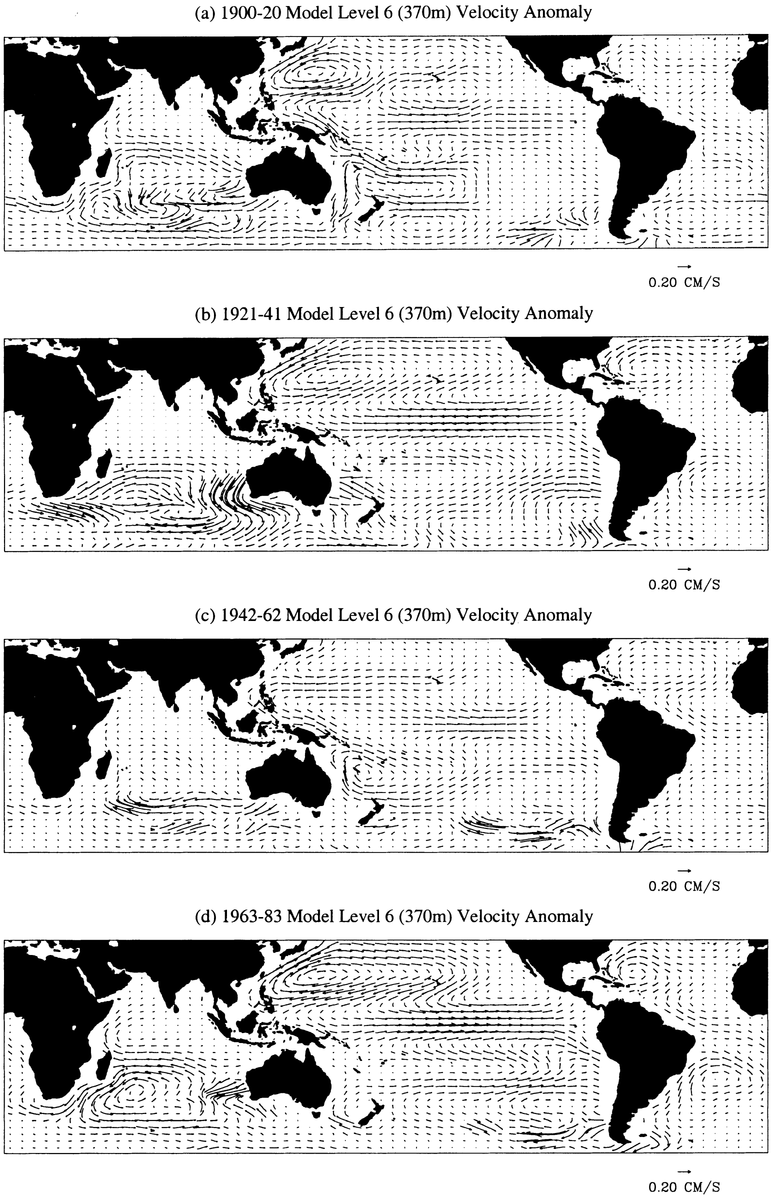

Fig. 9. As for Fig. 5 except perturbation currents at 370 m depth. A scale vector is shown.

relative to the western boundary or equatorial currents).

Thus, in the model at least, the observed multidecadal SST variability over most of the subtropical/mid-latitude Southern Hemisphere basins mainly arises from the epoch heat flux forcing (see Table 1 for summary). Only in the regions of the western boundary currents and their outflows into the central and western mid-latitudes of each Southern Hemisphere basin, do wind-driven dynamical effects make a large contribution. Dynamical effects are also important for the SST variability in the equatorial upwelling zones but these regions are not the main focus of this study.

Table 1. *Summary of major Southern Hemisphere regions of epoch SST variability and dominant contributing mechanisms*

Region	Mechanism
subtropics	Surface heat fluxes
western mid-latitudes	advection and surface heat fluxes
eastern mid-latitudes	surface heat fluxes
central mid-latitude South Pacific	surface heat fluxes and Ekman drift
equatorial upwelling zones	wind-driven upwelling

Note that advective effects in the western mid-latitudes of the Southern Hemisphere were weak during 1942–1962 since the wind stress changes over the subtropical gyre regions (Fig. 4c) are relatively small then. Wind-driven upwelling changes were most noticeable in the eastern to central equatorial Pacific and less obvious in the equatorial Atlantic.

These results suggesting the relative importance of surface heat flux versus wind stress forcing in different parts of the ocean basins appear consistent with previous studies that have applied various ocean models to investigate mechanisms of decadal and longer period climate variability in specific regions (Miller et al., 1994 in the North Pacific Ocean; Carton et al. 1996 in the tropical Atlantic Ocean).

5. Summary and discussion

Three sets of experiments have been performed with a coarse resolution global ocean general circulation model (OGCM) to investigate mechanisms of multidecadal SST variability in the subtropics and mid-latitudes of the Southern Hemisphere. These consist of the OGCM climatological forcing replaced by the observed variability in wind stress only, in net surface heat flux only, and in both wind stress and heat flux. When the only anomalous forcing is the wind stress variability so that only dynamical effects are included, the resulting model SST anomalies are most prominent in the regions of the western boundary currents and their outflows into the central and western mid-latitudes of each Southern Hemisphere basin. The mechanism involves modulation of the intensity of the subtropical gyre, and therefore in the transport of warm tropical waters into the southern mid-latitudes, in response to the variability in the winds. Smaller SST anomalies, associated with Ekman drift, were found in the central to eastern mid-latitude South Pacific. It is noted that there are also significant model SST anomalies in the equatorial upwelling zones (related to wind-driven changes in upwelling) but these are not dealt with in detail since these regions are not the main focus of this study.

When the anomaly forcing also included the epoch surface heat fluxes, so as to incorporate thermodynamic effects, the resulting model SST anomalies extend throughout the subtropics and mid-latitudes of each basin, and are more comparable in magnitude and pattern to the observed SST variability. Latent heat flux changes appear to dominate over sensible heat flux changes or advective effects in generating these model SST anomalies over much of the region. Only in the southern mid-latitudes, near the western boundary currents and their outflow regions, do advective effects make a large contribution to the subtropical/mid-latitude Southern Hemisphere SST variability. The experiments performed with the wind stress variability removed and only the surface heat flux anomalies included confirmed this result.

While an OGCM incorporating both the dynamic and the thermodynamic effect of the observed variability in near-surface wind, air temperature and derived humidity over the near-global tropical to mid-latitude ocean leads to SST anomalies that bear some resemblance to those observed, there are other factors which may also contribute in the real world. One such factor involves changes to the net radiative flux received at the ocean surface. In the current study, this term (R in eq. (1)) has been kept constant due to the less robust nature of, and numerous gaps in, the COADS cloud cover data, particularly for the earlier epochs and the Southern Hemisphere. However, it is certainly possible that there may have been substantial radiative flux anomalies during the epochs which if implemented in (1)–(3) could modify the model SST variability. By keeping R constant, the model has not been forced with any signal from the enhanced greenhouse gas effect which is consistent with the de-trending of the observed SST patterns (Fig. 1). However, there may be a greenhouse signal in the other forcing fields (COADS winds, air temperature, humidity) which, if removed, could lead to a closer correspondence between model and observed SST. The de-trending of SST using the leading EOF was not feasible with these other fields since the COADS data is gappy and less robust than the SST data (GISST2.2).

Other potential drawbacks of the current study that need to be mentioned are that seasonal effects are excluded and that the model is of coarse resolution. In terms of the former, it may be noted that there is little difference between the observed multidecadal fields when these are based on annual means (as shown in Figs. 1–4) as opposed to seasonal means. This result suggests that seasonal effects are unlikely to be of importance for variability on these multidecadal scales and a test experiment with the annual cycle resolved gave results which re-inforce the suggestion that these effects are not significant. Furthermore, there is little evidence in Fig. 1, or its 4 seasonal mean equivalents, of any concentration of SST gradients or other link with location of the seasonally reversing tropical currents associated with the monsoons in the Indian and western Pacific Oceans. Again, this suggests that using annual mean data is satisfactory on these long time scales. Regarding the resolution, tests with a model with twice as fine a grid showed no significant difference from those obtained with the current model. Over much of the central subtropics to mid-latitudes of each basin, where currents and hence eddy activity are relatively weak, it is suggested that lack of an eddy-permitting resolution is less likely to be significant. Indeed, the original COADS forcing data is considerably coarser than eddy resolution and trying to interpolate it to such a grid would be problematic. However, in regions such as the western boundary and equatorial zone, eddy activity in the real ocean is pronounced and it is possible that an eddy-permitting model could lead to different results if the problems of the forcing data and the huge computational expense (spin-up plus at least 4 epoch runs of 21 years each) could be overcome.

The implicit assumption behind this work, namely, that the observed atmospheric variability (Figs. 2–4) used to force the ocean model has itself arisen from a mechanism other than that due to forcing by the observed SST anomalies (Fig. 1) is supported by recent experiments with an atmospheric GCM. When forced with an idealized SST anomaly that stretches across the Southern Hemisphere mid-latitudes and which resembles the warming seen in this region during the 1963–1983 epoch (Fig. 1d), the atmospheric model response includes near-surface wind anomalies that are quite different to those shown in Fig. 4d. Instead, there is a pronounced weakening of the atmospheric model mid-latitude westerlies and a general reduction in the Southern Hemisphere trades rather than the strengthening seen in the observations (Fig. 4d). What may also be noted is that the observed wind stress variability (Fig. 4) appears to have somewhat of a wavenumber 3 structure in the subtropics, particularly during 1921–1941 and 1963–1983. Mean sea level pressure anomalies computed from a data set (GMSLP2.1f) other than the COADS used for the wind stresses (Fig. 4) indicate a weakening of the subtropical semi-permanent anticyclones over each Southern Hemisphere basin (and positive anomalies over the 3 landmasses) during 1900–1920 and particularly 1921–1941 with a strengthening of these anticyclones during 1963–1983 and to lesser extent 1942–1962 (Reason et al., 1998). This pattern is reminiscent of a wavenumber 3 pattern which after wavenumber 1 is the main component of the Southern Hemisphere circulation (van Loone and Jenne, 1972; Trenberth, 1979; Mo and White, 1985). It seems conceivable therefore that the atmospheric variability may be related to a process (e.g., differential long term warming of the Southern Hemisphere oceans versus the landmasses) that tends to modulate the prominence of wavenumber 3 in the Southern Hemisphere circulation. Since the Southern Hemisphere atmospheric circulation likes to show wavenumber 3 behaviour, it seems possible that this mode will be more sensitive to further excitation and that the multidecadal atmospheric variability could be related to changes in the magnitudes and/or zonal shifts in the location of this mode's ridges and troughs. Recent studies of the interannual Antarctic Circumpolar Wave (ACW) phenomenon using fully coupled models (Cai et al., 1999; Christoph et al., 1998) and an OGCM forced by ECMWF fluxes (Bonekamp et al., 1999), support the idea that wavenumber 3 can contribute significantly to low frequency variability in the Southern Hemisphere. Although the atmosphere is stochastic, its dominant modes with preferred spatial scales (wavenumber 3) can play an important rôle in Southern

Hemisphere variability on these long time scales, the low frequency of the variability being set by the ocean (Haarsma et al., 1999). It should also be noted that previous observational and modelling work (Krishnamurti et al., 1986; James and James, 1989; Karoly et al., 1995) has provided evidence of atmospheric variability on decadal and longer time scales that is not necessarily related to oceanic forcing. While determining the generation mechanism of the atmospheric component of the multidecadal variability has not been addressed here, it is clear from the foregoing that there is some justification for the approach adopted in this study of focussing on the oceanic response to this atmospheric variability.

Given that the ACW (White and Peterson, 1996) appears to involve a circumpolar propagation of anomalies in SST, sea–ice extent, mean sea level pressure and wind stress at latitudes not much different from the largest mid-latitude anomalies in the observed multidecadal SST variability (Fig. 1) as well as interaction with the subtropical gyres, it is natural to ask whether this prominent interannual mode may contribute in some way to what is observed on the multidecadal scale. This study cannot address that question but the following points may be made. Three important features of the observed ACW (White and Peterson, 1996; Peterson and White, 1998; White et al., 1998) are that there is a wavenumber 2 structure, that there appears to be a source region for the SST anomalies in the subtropical western Pacific immediately east of Australia (20–30°S, 150°E–150°W) and that there is a tilt in the alignment of the SST and MSLP anomalies such that the latter straddle the boundary between warm and cool anomalies around the Antarctic Circumpolar Current region. At mid-latitudes where the ACW signal should be more obvious, the observed SST (Fig. 1) and atmospheric variability (Figs. 2–4) shows little evidence of any ACW-like wavenumber 2 structure. Similarly, there is little evidence of any source existing in the subtropical western Pacific. These differences in the multidecadal variability from the ACW argue against the former being related to a direct compounding of the 4–5-year period of the ACW signal over the 21 years of each epoch although they do not negate the possibility of a more subtle influence of the ACW. However, what the ACW phenomenon and also the basic geography of the region indicate is that mechanisms of decadal to multidecadal variability in the Southern Hemisphere subtropics/mid-latitudes may well differ to some extent from those in the Northern Hemisphere. The lack of mid-latitude landmasses in the Southern Hemisphere not only enables the Antarctic Circumpolar Current to exist and thereby efficiently advect anomalies around the Southern Ocean but it also means that there are likely to be differences in surface heat flux exchange since there is not a comparable source of dry cold air during winter at subtropical to mid-latitudes as provided by Asia and North America for interaction with the western boundary currents. In the Southern Hemisphere, parent mid-latitude depressions tend to track at latitudes (Jones and Simmonds, 1993) south of the mid-latitude outflows of these currents and there is a less pronounced air mass exchange associated with the associated frontal systems during winter than is typical for Northern Hemisphere systems. These factors suggest that the generation and evolution of Southern Hemisphere decadal/multidecadal variability may well differ from that observed in the Northern Hemisphere.

6. Acknowledgements

I am indebted to GFDL for making the original code available and to Tony Hirst and co-workers who developed an earlier version of the global model used in this study from that code at CSIRO Atmospheric Research. Ross Murray, David Noone and Peter Otto assisted with data analysis for which I am very grateful. Partial funding for this study from the Australian Research Council and the South African Water Research Commission is gratefully acknowledged.

REFERENCES

Allan, R. J. and Haylock, M. R. 1993. Circulation features associated with the winter rainfall decrease in south-western Australia. *J. Clim.* **6**, 1356–1367.

Allan, R. J., Lindesay, J. A. and Reason, C. J. C. 1995. Multidecadal variability in the climate system over the Indian Ocean region during the austral summer. *J. Clim.* **8**, 1853–1873.

Anderson, D. L. T. and Willebrand, J. 1996 (eds.). *Deca-*

dal climate variability: dynamics and predictability. NATO ASI series, **44**, Springer-Verlag, Berlin, 493 pp.
Basnett, T. A. and Parker, D. E. 1997. *Development of the global mean sea level pressure data set GMSLP version 2.* United Kingdom Meteorological Office, Climate Research Tech. Note, 79, 16 pp.
Bonekamp, H., Sterl, A. and Komen, G. J. 1999. Interannual variability in the Southern Ocean from an ocean model forced by European Centre for Medium-Range Weather Forecast re-analysis fluxes. *J. Geophys. Res.* **104**, 13,317–13,331.
Bryan, K. 1969. A numerical method for the study of the circulation of the world ocean. *J. Comput. Phys.* **4**, 347–376.
Cai, W., Baines, P. G. and Gordon, H. B. 1999. Southern mid-to-high variability, a zonal wavenumber 3 pattern, and the Antarctic Circumpolar wave in a coupled model. *J. Clim.* **10**, 3087–3104.
Carton, J. A., Cao, X., Giese, B. S. and da Silva, A. M. 1996. Decadal and interannual variability in the tropical Atlantic Ocean. *J. Phys. Oceanogr.* **26**, 1165–1175.
Christoph, M., Barnett, T. P. and Roeckner, E. 1998. The Antarctic Circumpolar Wave in a coupled ocean–atmosphere GCM. *J. Clim.* **11**, 1659–1672.
Cox, M. D. 1984. *A primitive equation, 3-dimensional model of the ocean.* GFDL Ocean Group technical report no. 1, Princeton University.
Deser, C. and Blackmon, M. L. 1993. Surface climate variations over the North Atlantic Ocean during winter: 1900–1989. *J. Clim.* **6**, 1743–1753.
Esbensen, S. K. and Kushnir, Y. 1981. *The heat budget of the global ocean: an atlas based on estimates from surface marine observations.* Oregon State University Climate Research Institute report no. 29, 27 pp.
Giese, B. S. and Cayan, D. R. 1993. Surface heat flux parameterizations and tropical Pacific sea surface temperature simulations. *J. Geophys. Res.* **98**, 6979–6989.
Graham, N. E. 1994. Decadal-scale climate variability in the tropical and North Pacific during the 1970s and 1980s: observations and model results. *Clim. Dyn.* **10**, 135–162.
Haarsma, R. J., Selten, F. M. and Opsteegh, J. D. 1999. On the mechanism of the Antarctic circumpolar wave. *J. Clim.*, in press.
Hantel, M. 1970. Monthly charts of surface wind divergence over the tropical Indian Ocean. *Bonner Meteorologische Abhandlungen* **14**, 31–79.
Hellerman, S. and Rosenstein, M. 1983. Normal monthly windstress over the world ocean with error estimates. *J. Phys. Oceanogr.* **13**, 1093–1104.
Hirst, A. C. and Cai, W. J. 1994. Sensitivity of a world ocean GCM to changes in subsurface mixing parameterization. *J. Phys. Oceanogr.* **24**, 1256–1279.
James, I.N. and James, P.M. 1989. Ultra-low frequency variability in a simple atmospheric circulation model. *Nature* **342**, 53–55.
Jones, D.A. and Simmonds, I. H. 1993. A climatology of Southern Hemisphere extratropical cyclones. *Clim. Dyn.* **9**, 131–145.
Jones, P. D. and Allan, R. J. 1998. Climate change and long-term climatic variability. In: *Meteorology of the Southern Hemisphere* (eds. Karoly, D. and Vintcent, D.). Amer. Meteorol. Soc., Boston, Massachussets, pp. 337–363.
Karoly, D., Hope, P. and Jones, P. D. 1995. Decadal variations of the Southern Hemisphere circulation. *Int. J. Climatol.* **16**, 723–738.
Krishnamurti, T. N., Chu, S. H. and Islegias, W. 1986. On the sea level pressure of the Southern Oscillation. *Arch. Meteor. Geophys. Bioklimatol. Ser. A* **34**, 385–425.
Kushnir, Y. 1994. Interdecadal variations in North Atlantic sea surface temperature and associated atmospheric conditions. *J. Clim.* **7**, 141–157.
Latif, M. and Barnett, T. P. 1996. Decadal variability over the North Pacific and North America: dynamics and predictability. *J. Clim.* **9**, 2407–2423.
Levitus, S, 1982. Climatological atlas of the world ocean. *NOAA Professional Paper* **13**, US Govt. Printing Office, 173 pp.
Miller, A. J., Cayan, D. R., Barnett, T. P., Graham, N. E. and Oberhuber, J. M. 1994. Interdecadal variability of the Pacific Ocean: model response to observed heat flux and wind stress anomalies. *Clim. Dyn.* **9**, 287–302.
Mo, K. and White, G. H. 1985. Teleconnections in the Southern Hemisphere. *Mon. Wea. Rev.* **113**, 22–37.
Moore, A. M. and Reason, C. J. C. 1993. The response of a global ocean general circulation model to climatological surface boundary conditions for temperature and salinity. *J. Phys. Oceanogr.* **23**, 300–328.
Pacanowski, R. C., Dixon, K. and Rosati, A. 1991. *The GFDL modular ocean model users guide*, version 1.0. GFDL Ocean Group technical report no. 2, Princeton University.
Parker, D. E., Jones, P. D., Folland, C. K. and Bevan, A. 1994. Interdecadal changes of surface temperature since the late nineteenth century. *J. Geophys. Res.* **99**, 14,373–14,399.
Parker, D. E., Jackson, M. and Horton, E. B. 1995. *The GISST2.2 sea surface temperature and sea–ice climatology.* Clim. Res. Tech. Note, CRTN63, 35 pp. UK Met. Office, Bracknell, UK.
Peterson, R. G. and White, W. B. 1998. Slow oceanic teleconnections linking the Antarctic Circumpolar wave with the tropical El Nino–Southern oscillation. *J. Geophys. Res.* **103**, 24573–24583.
Reason, C. J. C., Allan, R. J. and Lindesay, J. A. 1996a. Dynamical response of the oceanic circulation and temperature to interdecadal variability in the surface winds over the Indian Ocean. *J. Clim.* **9**, 97–114.
Reason, C. J. C., Allan, R. J. and Lindesay, J. A. 1996b. Evidence for the influence of remote forcing on upper ocean temperature variability in the southern Indian Ocean. *J. Geophys. Res.* **101**, 11,867–11,882.
Reason, C. J. C., Allan, R. J. and Lindesay, J. A. 1998. Climate variability on decadal time scales: mechanisms and implications for climate change. *Palaeoclimates* **3**, 25–49.

Salinger, M. J., Allan, R. J., Bindoff, N., Hannah, J., Lavery, B., Lin, Z., Lindesay, J. A., Nicholls, N., Plummer, N. and Torok, S. 1996. Observed variability and change in climate and sea level in Australia, New Zealand and the South Pacific. In: *Greenhouse — coping with climate change* (eds. Bouma, W. J., Pearman, G. I. and Manning, M. R.). CSIRO Publishing, Collingwood, Victoria, pp. 100–126.

Schiller, A., Godfrey, J. S., McIntosh, P. C., Meyers, G. and Fiedler, R. 1999. Interannual dynamics and thermodynamics of the Indo-Pacific oceans. *J. Phys. Oceanogr.*, in press.

Trenberth, K. E. 1979. Interannual variability of the 500 mb zonal mean flow in the Southern Hemisphere. *Mon. Wea. Rev.* **107**, 1515–1524.

Trenberth, K. E. and Hurrell, J. W. 1994. Decadal atmosphere–ocean variations in the Pacific. *Clim. Dyn.* **9**, 303–319.

van Loon, H. and Jenne, R. L. 1972. The zonal harmonic standing waves in the Southern Hemisphere. *J. Geophys. Res.* **77**, 992–1003.

Venegas, S. A., Mysak, L. A. and Straub, D. N. 1996. Evidence for interannual and interdecadal climate variability in the South Atlantic. *Geophys. Res. Lett.* **23**, 2673–2676.

Ward, M. N. and Hoskins, B. J. 1996. Near-surface wind over the global ocean 1949–1988. *J. Clim.* **9**, 1877–1895.

White, W. B., Chen, S.-C. and Peterson, R. G. 1998. The Antarctic circumpolar wave: a beta-effect in ocean–atmosphere coupling over the Southern Ocean. *J. Phys. Oceanogr.* **28**, 2345–2361.

White, W. B. and Peterson, R. G. 1996. An Antarctic circumpolar wave in surface pressure, wind, temperature and sea–ice extent. *Nature* **380**, 699–702.

WMO, 1996. *World Climate Research Programme Workshop on air–sea flux fields for forcing ocean models and validating GCMs.* WCRP-95–WMO/TD no. 762, World Meteorological Organisation.

Woodruff, S. D. Slutz, R. J., Jenne, R. L. and Steurer, P. M. 1987. A comprehensive ocean–atmosphere data set. *Bull. Amer. Meteorol. Soc.* **68**, 1239–1250.